Full title:

Imputation of canine genotype array data using 365 whole-genome sequences improves power of genome-wide association studies

Short title:

Use of imputation in canine genome-wide association studies

Jessica J. Hayward[1]*, Michelle E. White[1], Michael Boyle[2], Laura M. Shannon[3], Margret L. Casal[4], Marta G. Castelhano[5], Sharon A. Center[5], Vicki N. Meyers-Wallen[1,6], Kenneth W. Simpson[5], Nathan B. Sutter[7], Rory J. Todhunter[5], Adam R. Boyko[1]

[1]Department of Biomedical Sciences, College of Veterinary Medicine, Cornell University, Ithaca, New York, United States of America

[2]Cornell Center for Astrophysics and Planetary Science, Cornell University, Ithaca, New York, United States of America

[3]Department of Horticultural Science, University of Minnesota, St Paul, Minnesota, United States of America

[4]School of Veterinary Medicine, University of Pennsylvania, Philadelphia, Pennsylvania, United States of America

[5]Department of Clinical Sciences, College of Veterinary Medicine, Cornell University, Ithaca, New York, United States of America

[6]Baker Institute for Animal Health, College of Veterinary Medicine, Cornell University, Ithaca, New York, United States of America

[7]Biology Department, La Sierra University, Riverside, California, United States of America

* Corresponding author

E-mail: jessica.hayward@cornell.edu (JJH)

Abstract:

Genomic resources for the domestic dog have improved with the widespread adoption of a 173k SNP array platform and updated reference genome. SNP arrays of this density are sufficient for detecting genetic associations within breeds but are underpowered for finding associations across multiple breeds or in mixed-breed dogs, where linkage disequilibrium rapidly decays between markers, even though such studies would hold particular promise for mapping complex diseases and traits. Here we introduce an imputation reference panel, consisting of 365 diverse, whole-genome sequenced dogs and wolves, which increases the number of markers that can be queried in genome-wide association studies approximately 130-fold. Using previously genotyped dogs, we show the utility of this reference panel in identifying novel associations and fine-mapping for canine body size and blood phenotypes, even when causal loci are not in strong linkage disequilibrium with any single array marker. This reference panel resource will improve future genome-wide association studies for canine complex diseases and other phenotypes.

Author Summary:

Complex traits are controlled by more than one gene and as such are difficult to map. For complex trait mapping in the domestic dog, researchers use the current array of 173,000 variants, with only minimal success. Here, we use a method called imputation to increase the number of variants – from 173,000 to 24 million – that can be queried in canine association studies. We use sequence data from the whole genomes of 365 dogs and wolves to accurately predict variants, in a separate cohort of dogs, that are not present on the array. Using dog body size, we show that the increase in variants results in an increase in mapping power, through the identification of new associations and the narrowing of regions of interest. This imputation panel is particularly important because of its usefulness in improving complex trait mapping in the dog, which has significant implications for discovery of variants in humans with similar diseases.

Introduction:

The modern domestic dog (*Canis lupus familiaris*) consists of over 500 breeds selected for diverse roles and subject to wildly different disease prevalences (1). A high quality reference genome (2–4) and affordable SNP genotyping arrays (5) have helped make the dog a powerful animal model for studying the genetics of complex traits and diseases. Of 719 traits genetic traits and disorders in the dog, 420 are potential models of human disease (https://omi.org/home/). With an average spacing of 1 SNP every 13kb, the CanineHD array (Illumina, San Diego, CA) has been successfully implemented in many genome-wide association studies (GWAS), especially within single breeds where linkage disequilibrium (LD) often extends beyond 1Mb (for example, see (6,7)). However, the results of many complex disease mapping studies in dogs have been underwhelming, with only one or a few significant loci identified (for example, see (8–10)). 57% of the 719 genetic traits and disorders in dogs are complex but the likely causal variant is known for only 27% of these (https://omia.org/home/).

Recently, we used simulations to show that an increase in SNP density to 1 SNP every 2kb would improve power for canine complex trait GWAS (8). An increase in density can be achieved by the following: adding more SNPs to the CanineHD array, using whole genome sequencing (WGS), or using imputation to predict genotypes through the use of a reference panel created from WGS data. Of these, imputation is the most cost-effective option and has been used successfully in human and cattle GWAS, especially with the recent WGS efforts in these species (11,12).

GWAS of canine morphological traits has been very successful, due to large effect sizes and long regions of LD as a result of recent selection in purebred dogs (13). Seventeen quantitative trait loci (QTLs) associated with body weight, as a proxy for body size, have been identified (5,8,14–22), as well as associations for other morphological phenotypes such as ear flop (5,15,16) and fur type (8,23,24). Despite the success of morphological trait mapping, we suggest that imputation can improve the power of GWAS, especially for reducing large intervals for use in fine-mapping. We posit that improving the density of variants by using an imputation panel will greatly improve the power to identify causal loci for canine complex traits, due to increased LD. We use 365 canine whole genome sequences to create a reference panel of 24 million variants and impute these variants in 6,112 dogs previously genotyped on a semi-custom 185k CanineHD array. We

84 show that using an imputation panel increases our power to detect variants affecting complex
85 canine traits – both morphological and blood phenotypes – by identifying novel loci, and by
86 refining intervals for previously-identified QTL's for use in fine-mapping. To our knowledge, this is
87 the first study to use an imputation panel based on WGS for canine mapping studies.
88
89 **Results**:
90 Evaluation of imputation accuracy
91 We used IMPUTE2 to impute the WGS reference panel across the 6,112 genotyped dogs
92 resulting in 24 million variants. By comparing 33,144 imputed variants to directly genotyped sites
93 on a second custom array, we were able to calculate the accuracy for our imputation panel, which
94 was 88.4% overall. Across all sites, purebred dogs had the highest accuracy (89.7%, n=276),
95 followed by mixed-breed dogs (88.6%, n=13), and then village dogs (84.2%, n=86). This result is
96 expected given that 210 of our 365 WGS panel were purebred dogs, and also due to the long-
97 range haplotypes found in purebreds that make calling imputed variants easier. For all three dog
98 types (purebred, mixed-breed, and village), imputation accuracy increased with decreasing minor
99 allele frequency (MAF) (Fig. 1a), which is an expected result because as MAF decreases, the
100 occurrence of the major allele is the correct call more often. Looking at true heterozygous sites
101 only (Fig. 1b), imputation accuracy was lower across all MAFs compared to all sites (Fig. 1a).
102 Imputation accuracy increased as MAF increased for heterozygous sites, as there are more
103 heterozygous calls for SNPs with higher MAF.
104 In general, the larger chromosomes and chromosome X had higher imputation accuracies than
105 the smaller chromosomes, such as 35, 36, 37, and 38, due to lower recombination rates (S1
106 Table). For all purebred, mixed-breed, and village dogs, the average imputation accuracy per
107 chromosome was 89.1% (range of 84.3-93.5%), 88.0% (range of 83.0-93.0%), and 83.7% (range
108 of 78.5-92.4%), respectively.
109
110 Body size associations

We performed two separate GWAS, firstly using the semi-custom CanineHD array data of 185k markers, and secondly using our imputed panel of 24 million variants. The phenotypes used in these GWAS were male breed-average weight$^{0.303}$, male breed-average height, and individual sex-corrected weight$^{0.303}$. We were then able to compare the results from the array GWAS and the imputed GWAS using the exact same phenotypes.

Using imputed data generally increased the significance of body size associations seen in the array data, especially *HMGA2* on CFA10 and fgf4 on CFA18 for height (Fig 2a,b,c; S2 Table). Most of the respective QTLs from the array GWAS and the imputed GWAS were in LD ($r^2 > 0.2$) with the exception of the CFA12 and two CFA26 associations (Table 1). When imputed variants were not in high LD ($r^2 < 0.8$) with array QTLs, the imputed variants generally had stronger effect sizes and lower minor allele frequencies (Table 1).

For most size-associated variants, the breed-average weight and height effects were roughly isometric, with the exception of CFA18 and CFA12 QTLs, which had a greater effect on height than weight (Fig. 2d). Of the seventeen autosomal QTLs that have been previously associated with body size (5,8,14–22,25), only one (CFA3:62) did not reach significance using the imputed panel (significance threshold of $P = 1\times10^{-8}$), with *P*-values of 1.1×10^{-5}, 2.1×10^{-7} and 1.8×10^{-8} for individual weight, breed-average weight and breed-average height respectively (S2 Table). GWAS of breed-average weight provided the most power on average, so we will focus on that phenotype for the rest of the body size analyses.

We used the identified body size QTLs to predict the body weight of individuals, by randomly setting 20% of the body weights in the dataset to missing, then using a Bayesian sparse linear mixed model to predict the missing weights, and finally comparing the predicted weights to the actual weights. Using the 20 QTLs identified from the array GWAS (see bold in Table 1), we found a correlation coefficient (r) of 0.851. Using the 20 QTLs from the imputed GWAS (see bold in Table 1), we found r of 0.869, and this increased very slightly to 0.870 when two more QTLs were included (see italics in Table 1).

Table 1: Positions, minor allele frequencies (MAF), and effect sizes for SNPs associated with breed-average male weight$^{0.303}$ using the array data and imputed data, and LD between these pairs of SNPs.

Chr	Array Position	Array MAF	Array Effect size	Imputation Position	Imputation MAF	Imputation Effect size	LD (r^2)
1	**55983871**	0.129	-0.071	**55922563**	0.127	-0.077	0.874
3	**41758863**	0.311	-0.031	**41780841**	0.111	-0.074	0.246
3	**62042184**	0.100	0.062	61887587	0.093	0.065	0.849
3	**91103945**	0.227	0.067	**91110878**	0.283	0.094	0.433
	91103945			*91138480*	0.237	0.045	0.088
4	**39112085**	0.334	-0.052	**39182836**	0.262	-0.060	0.396
4	**67026055**	0.404	-0.033	**67040898**	0.363	-0.074	0.382
5	**31895829**	0.461	-0.029	**31689208**	0.248	-0.045	0.265
7	**30243851**	0.271	-0.044	**30183217**	0.176	-0.067	0.518
7	**41392649**	0.356	-0.041	**41351722**	0.349	-0.044	0.903
7	**43719549**	0.382	-0.067	**43724293**	0.356	-0.076	0.894
9	N/A			**12034947**	0.054	-0.094	N/A
10	**8183593**	0.209	-0.135	**8379634**	0.249	-0.191	0.557
	8183593			*8100754*	0.194	-0.079	0.851
11	**26929946**	0.243	-0.045	**26929946**	0.243	-0.045	1.000
12	**33733595**	0.435	0.026	33712492	0.161	0.067	0.148
15	**41221438**	0.465	-0.115	**41216098**	0.464	-0.114	0.979
18	**20272961**	0.151	-0.083	**20379945**	0.161	-0.116	0.577
20	**21479863**	0.085	0.056	**21686712**	0.110	0.072	0.493
26	**7631562**	0.340	0.031	**7679257**	0.175	0.059	0.075
26	**13224865**	0.307	-0.042	**12838979**	0.232	-0.078	0.154
32	N/A			**5228269**	0.164	-0.077	N/A
34	**18559537**	0.237	-0.050	**18587956**	0.258	-0.051	0.849
39	**102212242**	0.345	0.073	**102209680**	0.342	0.075	0.983

20 array QTLs and 20 imputed QTLs (shown in bold) were used in a prediction model and then another 2 imputed QTLs (shown in italics) were added to the prediction model (see text).

Known body size loci

Nine body size QTLs have previously been fine-mapped (*IGF1R*, *STC2*, *GHR*, *SMAD2*, *HMGA2*, *FGF4*, *IGF1*, fgf4, *IGSF1*) (17–20,25,26). For each of these, the region in LD with the most significant respective marker in the breed-average weight imputed GWAS contained the known or putative causal variant (S1 Fig.). While the putative causal variants weren't always the highest associated variant at a locus, they generally had *P*-values within two orders of magnitude of the most associated marker (S1 Fig.), confirming that the imputation panel performs well for the weight GWAS.

Unsurprisingly, many of the putative causal variants are not markers on the CanineHD array, including *IGF1R* (3:41,849,479) (20), *STC2* (4:39,182,836), *GHR* (4:67,040,898 and 4:67,040,939), and *HMGA2* (10:8,348,804) (17). With the array data, the *IGF1R* QTL ($P = 1.4\times10^{-5}$ for breed-average weight GWAS) did not reach significance, but with the imputed data we saw a significant association signal ($P = 1.6\times10^{-12}$ for breed-average weight GWAS), and the causal variant was the 6th most associated SNP ($r^2 = 0.73$ between causal and associated SNP) (S1 Fig. a). The *STC2* and *GHR* (4:67,040,898) putative causal variants were the most significant variants at those loci in the imputed GWAS (S1 Fig. b,c). Note that there are two putative causal variants for *GHR* (17), both in exon 5, but only one passed our 5% MAF filter. Similarly, the *HMGA2* causal variant was in high LD (r^2=0.91) with the most significant marker at this locus in the imputed GWAS (S1 Fig. e).

For *IGF1*, SNP5 (BICF2P971192, 15:41,221,438), which is in LD with the SINE element (18), was the most significant association in the array GWAS. In the imputed GWAS, SNP5 was the 2nd most associated SNP and the SNP that tags the SINE element (15:41,220,982) was the 4th most associated SNP, and these SNPs were nearly in complete LD with the most significant marker in the GWAS (r^2=0.98 and 0.97 respectively) (S1 Fig. f). The *IGSF1* missense mutation (26) was in high LD with the most significant association in the imputed GWAS (r^2=0.97) (S1 Fig. i). Note that there is a second variant in *IGSF1* – an in-frame deletion – that has also been identified (26).

Imputed GWAS novel body size loci

We previously identified four novel QTLs, making a total of seventeen, that are associated with body size in dogs (8). Here, using the imputation data, we found a further five novel QTLs (CFA5:31, CFA7:41, CFA9:12, CFA26:7, CFA32:5) that passed our significance threshold in a breed-average weight GWAS. As a conservative control, we performed a further breed-average weight GWAS in which we included the four most-associated QTLs (CFA10:8, CFA15:41, CFA3:91, CFA7:43) as covariates. The results showed that the novel loci at CFA5:31, CFA7:41 and CFA32:5 were no longer significant – and four other loci were also not significant in the covariate GWAS: CFA1:56, CFA11:26, CFA20:21, CFA34:18. Further analyses are required to determine if these are true or spurious associations, but since we cannot rule out that they are spurious, we conclude that we have identified only two novel canine body size QTLs, at CFA9:12 and CFA26:7.

The most significant SNP at CFA9:12 is located about 200kb upstream of the gene *growth hormone 1* (*GH1)* (Fig. 3a), which is expressed in the pituitary and has been associated with body size in humans and cattle (27–29). The non-reference, derived indel that was the most highly associated in our imputed GWAS is found at high frequency in two small breeds Papillon and Pomeranian, and also in New Guinea Singing Dogs. Using our snpEff annotated variant files, we found two variants in *GH1*: a splice donor variant in intron 3 (CFA9:11,833,343, c.288+2_288+3insT), and an in-frame deletion in exon 5 (CFA9:11,832,437, c.573_578delGAAAGA, p.Lys191_Asp). Both of these variants were at <5% frequency in the WGS panel but all occurrences were in small-sized breeds (such as Yorkshire terrier and Maltese).

The second novel body size QTL is at CFA26:7 (Fig. 3b). Investigation of the surrounding region uncovered a couple of potential candidate genes. The first is *ANAPC5*, a member of the anaphase-promoting complex gene family that includes *ANAPC13*, which has been associated with height in humans (30). The second candidate gene is the histone H3 demethylase *KDM2B* (*lysine-specific demethylase 2B)*, which has been associated with body mass index in humans in a CpG methylation study (31). However, we did not identify any variants in *ANAPC5* or *KDM2B* in

198 the snpEff-annotated files that are in LD with the associated imputation variant. The non-
199 reference, derived allele was found at high frequency in the small breeds Shiba Inu, Havanese,
200 and Chihuahua.
201
202 Refinement of body size loci
203 With the imputation panel, we saw a refinement in several QTL regions – for example, the
204 chromosome 3 association near the genes *LCORL* and *ANAPC13,* both of which have previously
205 been associated with body size (5,15,29,30,32). Using imputed data, this QTL had a more
206 significant and defined association, compared to the CanineHD array data alone (S2 Fig. a). The
207 QTL interval is about 65kb and 60kb upstream of the genes *LCORL* and *ANAPC13* respectively,
208 suggesting the causal variant is likely regulatory. Another example is the recently identified body
209 size QTL at CFA7:30 Mb, near the gene *TBX19* (8). Here the imputed GWAS results showed a
210 narrower QTL interval of greater significance when compared to the array GWAS (S2 Fig. b). This
211 region overlaps *TBX19* but we did not observe any coding loci in our snpEff annotated variant
212 files that are in LD with the most associated SNP.
213
214 Allelic heterogeneity
215 In order to reduce phenotypic noise, again we included the four most-associated QTLs (CFA10:8,
216 CFA15:41, CFA3:91, CFA7:43) as covariates in the GWAS (hereafter referred to as “top 4
217 covariates”), and then implemented a region-specific stepwise approach, including further
218 associated SNPs in the region as covariates, until no significant association signal remained. For
219 breed-average body weight, when we regressed out the most significant association for a QTL,
220 we expected the association signal to disappear, as seen with the *SMAD2* QTL (Fig. 4a).
221 Our results showed two QTLs (CFA3:91, CFA10:8) that retain significant association signal after
222 regressing out the most associated locus in the respective region (Fig. 4b,c). For both CFA3 and
223 CFA10, the data suggest there may be two independent significant associations in these regions.
224 In the CFA3 region, the initial association signal peak looked regulatory while the residual signal
225 is located in the genes *ANAPC13* and *LCORL*. The residual signal in the CFA10 region lies close

to the ear flop association (5,15,16) (candidate gene *MSRB3*) but is not in LD with the imputed ear flop locus at CFA10: 8,097,650 (r^2=0.147). The variant in this residual signal region may be regulatory, as the significance peak lies approximately 248kb upstream of *HMGA2*. We did not identify any coding variants in these two residual signal regions from the snpEff annotations. Two other QTLs (CFA4:67 and CFA15:41) showed evidence of residual signal but these did not reach significance ($P = 2.9\times10^{-7}$ and 2.9×10^{-8}, respectively).

This residual signal suggested allelic heterogeneity in these regions but could also be due to imperfect tagging in the imputed dataset. As a follow-up analysis, for each of these two QTLs (CFA3:91 and CFA10:8), we took the most significant SNP from the top 4 covariates GWAS. We used that significant SNP as a covariate in a GWAS to see if we were able to recover the most significant SNP from the initial GWAS with no covariates. For both CFA3 and CFA10, we did recover the initial associated SNP, suggesting that these are real associations and not midway between two imperfectly tagged SNPs.

Blood phenotypes

Using our imputed panel for GWAS on blood phenotypes revealed several novel associations. For example, we saw significant associations with the phenotypes of albumin and calcium levels in peripheral blood ($P = 4.5\times10^{-10}$ and 5.9×10^{-9} respectively), neither of which were previously identified in the array GWAS (33) (S3 Table). We also identified a novel association with blood glucose level and CFA1, located in the gene solute carrier family 22 member 1 (S*LC22A1)* and about 30kb downstream of the insulin-like growth factor 2 receptor gene *(CI-MPR/IGF2R)* (Fig. 5d). During gestation, *IGF2R* binds insulin-like growth factor 2 (IGF2), the presence of which stimulates the uptake of glucose (34). The SNP was at highest frequency (>50%) in the Samoyed and American Eskimo dog breeds.

Of the eight significant associations (using a threshold of $P = 1.0\times10^{-8}$) we saw with the imputed data, only two were not novel – alanine aminotransferase (ALT) and amylase – although both increased in significance (Fig. 5g, 5h; S3 Table). In addition to significant associations, we also

saw six associations that nearly meet our significance threshold, that is, $P < 2.0\times10^{-8}$, including three that were not significant using the genotype data (S3 Table).

Discussion:

Imputation increases GWAS power by including additional sites that are not well-tagged by any single array marker, and has been successfully implemented in human studies, for example, low-density lipoprotein GWAS (35–37). Here we present a canine imputation panel of 24 million variants – an approximate 130-fold increase in SNP number and SNP density from the semi-custom CanineHD array – for use in association studies. This panel has an overall accuracy rate of 88.4% when compared to genotype data from the same individuals (276 purebreds, 86 village dogs, and 13 mixed-breed dogs). In the future, panels based on even larger numbers of sequenced individuals would yield even higher accuracy (for example, see (38)), but this panel based on hundreds of dogs is still a useful, cost-effective way to improve the power of canine mapping studies today.

With our imputation panel, we improved association mapping for previously studied phenotypes, such as body size. Previous mapping studies of canine body size and other morphological traits using CanineHD array data have identified many significant QTLs. This success is largely the result of selection for body size during the formation of dog breeds, leading to selective sweeps around large-effect loci that facilitated mapping efforts. Nevertheless, using the imputation panel, we were able to identify two additional novel loci (at CFA9:12 and CFA26:7) that influence body size although functional studies, which are beyond the scope of this research study, are required to validate these two loci. Using imputation, we were also able to narrow intervals for previously known associated QTLs, and find evidence of possible allelic heterogeneity at two loci. Furthermore, imputation provides a more accurate analysis of the genetic architecture underlying canine body size and, in turn, allows a more accurate prediction for body size in dogs.

Imputation is especially helpful in across-breed and/or mixed-breed study designs, where LD breaks down very rapidly making it more difficult to identify associations. Increasing the number and density of queried variants (as done by imputation) increases the chance that a variant will be

in LD with the causal variant, especially when compared to a within-breed study design. We used our imputation panel for across-breed GWAS of blood phenotypes, resulting in several novel associations and the narrowing of associated intervals when compared to array data alone. Although costs of WGS are decreasing, it is still more cost-effective to use a panel of WGS individuals to create an imputation dataset based on genotyped samples than it is to directly WGS all the samples (39). Our imputation panel was created using over 350 canine WGS's representing 76 breeds. The inclusion of more breeds, especially diverse breeds (such as the Parson Russell Terrier) and rare breeds (such as the Pumi), will improve the accuracy of, and the number of rare variants in, future imputation panels. A recent canine imputation study has shown that imputation accuracy is highest using a multi-breed reference panel (compared to a breed-specific panel), and when there is overlap in breeds between the target and reference panel (40). Furthermore, human studies have shown that imputation accuracy increases with the size of the reference panel (41,42).

In summary, using our canine imputation panel of 24 million variants results in an increase in GWAS power, even for phenotypes that have multiple significant associations. The improvements to canine GWAS, especially for complex phenotypes, will not only further the field of canine genetics, but may also have beneficial implications for human medical genetics – especially for complex diseases, such as cancer, for which the domestic dog is a good model organism (43).

Material and Methods:

Whole genome sequences

The 365 whole genome sequences include 210 breed dogs (from 76 breeds), 107 village dogs (from 13 countries), and 28 wolves (S4 Table). 88 of these were sequenced at the Cornell University BRC Genomics Facility; others were sourced from public databases (S4 Table). Those sequenced at Cornell were run on an Illumina HiSeq2000 or Illumina HiSeq2500 and the reads were aligned to the CanFam3.1 reference genome using BWA (44). Variants were called using GATK's HaplotypeCaller (46–48). Variant quality recalibration was done in GATK using the semi-custom canineHD variant sites (8) as a training set (known=false, training=true, truth=true,

prior=12.0). We included SNPs in the 99.9% tranche and removed sites with minor allele frequency (MAF) less than 0.5%. Phasing was done using Beagle r1399 (45).

Imputation panel

SHAPEIT v2.r790(49) was used to phase the genotype data from 6,112 dogs as previously described (8) and then IMPUTE2 version 2.3.0 (50) was used to impute across these data. Imputation was only performed on the autosomes and chromosome X, not on the Y chromosome or mitochondrial SNPs. The final reference panel consists of 24.0 million variants, including 750,000 on the X chromosome, of which 20.33 million are SNPs and 3.67 million are indels.

Imputation Accuracy

276 purebred, 86 village, and 13 mixed-breed dogs were also genotyped on a second custom Illumina CanineHD 215k array, which contains 33,144 SNPs that are not on the 185k semi-custom CanineHD array but do feature in our imputed dataset. These 33,144 SNPs were used to determine the accuracy of our imputation across the 375 total dogs. Accuracy was calculated for each SNP as the number of sites that are correctly called in the imputed dataset divided by the total number of dogs. For example, if a G/C SNP was called G/G in 14 dogs, C/C in 10 dogs, and G/C in the remaining 351 dogs, then the imputation accuracy for that SNP is 93.6%. MAF was calculated for each SNP as the number of occurrences of the allele across all village, purebred, and mixed-breed dogs in the genotyped dataset. Imputation accuracy and MAF were plotted in Jupyter notebook (51) using Matplotlib library (52).

Marker Datasets

For the genotype data, individuals were run on a semi-custom Illumina CanineHD array of 185k SNPs, and quality control steps were performed as previously described(8). For the imputed data, IMPUTE2 outputs were converted into PLINK (53) binary format, one for each chromosome.

GWAS

We ran GWAS using a linear mixed model in the program GEMMA v 0.94 (54), with a MAF cut-off of 5% and using the Wald test to determine *P*-values. All LD plots were created using Matplotlib library (52) in Jupyter notebook (51).

For the imputed panel, GWAS was performed for each canine chromosome (CFA1-39) separately. The kinship matrix calculated using the array data in GEMMA was also used in the imputed GWAS for the same phenotype. The significance threshold was set to $P = 1\times10^{-8}$ (see (55)).

1. Body size

To identify QTLs associated with body size, we ran a GWAS of breed-average body weights (n=1926) and heights (n=1926), and individual body weights (n=3095), using both the semi-custom 185k CanineHD array data and the imputed panel data. Effect sizes were recorded from the GEMMA output, and MAF's and LD statistics were calculated using PLINK.

Breed-average body size

The breed-average data included dogs from 175 breeds with a maximum of 25 dogs per breed. The phenotypes of male breed-average weight$^{0.303}$ in kg, or male breed-average height in cm, were assigned to all dogs in the breed for the weight and height GWAS, respectively. We used weight$^{0.303}$ to normalize the distribution of weights across the breeds, based on a Box-Cox transformation performed in R (56) using the package MASS (57).

Individual body weights

Individual body weight GWAS was performed using 3,095 dogs including 417 village dogs and 427 mixed-breed dogs. The average raw weight in this individual dataset is 24.7kg, ranging from 1.6kg to 99.7kg. 164 breeds are represented, with 52 small breeds, 57 medium breeds, 34 large, and 21 giant breeds. Individual weights were sex-corrected by 16.47% (that is, female weights were increased by 16.47%), and transformed (weight$^{0.303}$).

Covariate GWAS

GWAS of breed-average body weight using imputed variants shows the four most-associated loci are *HMGA2* (CFA10), *IGF1* (CFA15), *LCORL* (CFA3), and *SMAD2* (CFA7). In order to control for possible spurious associations, we ran an imputed GWAS, using breed-average body weights,

365 including the four most-associated loci as covariates and then observed which of our significant
366 associations remained.

367 *Fine mapping*

368 We used snpEff version 4.3T (58) to annotate our WGS variant file, using the pre-built
369 CanFam3.1.86 database, and then used this to search for potential causal variants within specific
370 LD regions.

371 *Predicting body size*

372 We used all the individual body weights (n=3,095) and specific body size QTLs as a training set,
373 and then randomly set 20% of the weights to missing and used a Bayesian sparse linear mixed
374 model (with a ridge regression/GBLUP fit) in GEMMA to predict these missing weights. We did
375 this randomization and prediction 50 times, and then compared the actual weights to the
376 predicted weights using a correlation coefficient.

377 *Allelic heterogeneity*

378 In order to reduce phenotypic noise, we again included all four most-associated QTLs as
379 covariates in a follow-up GWAS of breed-average body weight and then, for those regions that
380 still had residual association signal, we also included the most associated SNP (in addition to the
381 four) as a covariate in the next GWAS. We continued this stepwise process of including the most-
382 associated SNP in the next GWAS until there was no significant association signal in the
383 respective region remaining. The same analysis was run using the three most-associated loci
384 (*HMGA2, IGF1, LCORL*) and the five most-associated loci (*HMGA2, IGF1, LCORL, SMAD2,*
385 *GHR*) with comparable results (data not shown).

386 2. Blood phenotypes

387 Using previously published data of 38 phenotypes from complete blood count (CBC) and serum
388 chemistry diagnostic panels (33), GWAS were performed using the imputed data and results
389 were compared to the published results using the semi-custom CanineHD array data.

390

391 Data Availability

Whole-genome sequence data produced for this research have been deposited in the Sequence Read Archive (http://www.ncbi.nlm.nih.gov/sra) with accession numbers listed in S4 Table. The pre-phased genotype data (binary PLINK files) and the phased WGS data (vcf files) are publicly available at datadryad.org (doi:10.5061/dryad.jk9504s).

Acknowledgments:

The authors would like to acknowledge Liz Corey and other Cornell Veterinary Biobank personnel, Peter Schweitzer at the Cornell University Genomics Facility, and the many dog owners that contributed samples.

Author Contributions:

Investigation: JJH, ARB

Formal analysis: MB, LMS

Resources: MEW, MLC, MGC, SAC, VM-W, KWS, NBS, RJT

Writing – original draft preparation: JJH, ARB

Writing – review and editing: JJH, MEW, MB, LMS, MLC, MGC, SAC, VM-W, KWS, NBS, RJT, ARB

Competing financial interests:

ARB is the chief scientific officer of Embark Veterinary Inc.

References

1. Asher L, Diesel G, Summers JF, McGreevy PD, Collins LM. Inherited defects in pedigree dogs. Part 1: Disorders related to breed standards. Vet J. 2009 Dec;182(3):402–11.

2. Lindblad-Toh K, Wade CM, Mikkelsen TS, Karlsson EK, Jaffe DB, Kamal M, et al. Genome sequence, comparative analysis and haplotype structure of the domestic dog. Nature. 2005 Dec 8;438(7069):803–19.

3. Hoeppner MP, Lundquist A, Pirun M, Meadows JRS, Zamani N, Johnson J, et al. An Improved Canine Genome and a Comprehensive Catalogue of Coding Genes and Non-Coding Transcripts. PLOS ONE. 2014 Mar 13;9(3):e91172.

4. Kirkness EF, Bafna V, Halpern AL, Levy S, Remington K, Rusch DB, et al. The Dog Genome: Survey Sequencing and Comparative Analysis. Science. 2003 Sep 26;301(5641):1898–903.

5. Vaysse A, Ratnakumar A, Derrien T, Axelsson E, Pielberg GR, Sigurdsson S, et al. Identification of Genomic Regions Associated with Phenotypic Variation between Dog Breeds using Selection Mapping. PLOS Genet. 2011 Oct 13;7(10):e1002316.

6. Wolf ZT, Brand HA, Shaffer JR, Leslie EJ, Arzi B, Willet CE, et al. Genome-Wide Association Studies in Dogs and Humans Identify ADAMTS20 as a Risk Variant for Cleft Lip and Palate. PLOS Genet. 2015 Mar 23;11(3):e1005059.

7. Tengvall K, Kierczak M, Bergvall K, Olsson M, Frankowiack M, Farias FHG, et al. Genome-Wide Analysis in German Shepherd Dogs Reveals Association of a Locus on CFA 27 with Atopic Dermatitis. PLOS Genet. 2013 May 9;9(5):e1003475.

8. Hayward JJ, Castelhano MG, Oliveira KC, Corey E, Balkman C, Baxter TL, et al. Complex disease and phenotype mapping in the domestic dog. Nat Commun. 2016 Jan 22;7:10460.

9. Mogensen MS, Karlskov-Mortensen P, Proschowsky HF, Lingaas F, Lappalainen A, Lohi H, et al. Genome-Wide Association Study in Dachshund: Identification of a Major Locus Affecting Intervertebral Disc Calcification. J Hered. 2011 Sep 1;102(Suppl_1):S81–6.

10. Quilez J, Martínez V, Woolliams JA, Sanchez A, Pong-Wong R, Kennedy LJ, et al. Genetic Control of Canine Leishmaniasis: Genome-Wide Association Study and Genomic Selection Analysis. PLOS ONE. 2012 Apr 25;7(4):e35349.

11. Daetwyler HD, Capitan A, Pausch H, Stothard P, van Binsbergen R, Brøndum RF, et al. Whole-genome sequencing of 234 bulls facilitates mapping of monogenic and complex traits in cattle. Nat Genet. 2014 Aug;46(8):858–65.

12. The 1000 Genomes Project Consortium. A global reference for human genetic variation. Nature. 2015 Oct 1;526(7571):68–74.

13. Karlsson EK, Lindblad-Toh K. Leader of the pack: gene mapping in dogs and other model organisms. Nat Rev Genet. 2008 Sep;9(9):713–25.

14. Eigenmann JE, Patterson DF, Froesch ER. Body size parallels insulin-like growth factor I levels but not growth hormone secretory capacity. Acta Endocrinol (Copenh). 1984 Aug;106(4):448–53.

15. Boyko AR, Quignon P, Li L, Schoenebeck JJ, Degenhardt JD, Lohmueller KE, et al. A Simple Genetic Architecture Underlies Morphological Variation in Dogs. PLOS Biol. 2010 Aug 10;8(8):e1000451.

16. Jones P, Chase K, Martin A, Davern P, Ostrander EA, Lark KG. Single-Nucleotide-Polymorphism-Based Association Mapping of Dog Stereotypes. Genetics. 2008 Jun;179(2):1033–44.

17. Rimbault M, Beale HC, Schoenebeck JJ, Hoopes BC, Allen JJ, Kilroy-Glynn P, et al. Derived variants at six genes explain nearly half of size reduction in dog breeds. Genome Res. 2013 Dec;23(12):1985–95.

18. Sutter NB, Bustamante CD, Chase K, Gray MM, Zhao K, Zhu L, et al. A single IGF1 allele is a major determinant of small size in dogs. Science. 2007 Apr 6;316(5821):112–5.

19. Parker HG, VonHoldt BM, Quignon P, Margulies EH, Shao S, Mosher DS, et al. An Expressed Fgf4 Retrogene Is Associated with Breed-Defining Chondrodysplasia in Domestic Dogs. Science. 2009 Aug 21;325(5943):995–8.

20. Hoopes BC, Rimbault M, Liebers D, Ostrander EA, Sutter NB. The insulin-like growth factor 1 receptor (IGF1R) contributes to reduced size in dogs. Mamm Genome Off J Int Mamm Genome Soc. 2012 Dec;23(11–12):780–90.

21. Chase K, Carrier DR, Adler FR, Jarvik T, Ostrander EA, Lorentzen TD, et al. Genetic basis for systems of skeletal quantitative traits: Principal component analysis of the canid skeleton. Proc Natl Acad Sci. 2002 Jul 23;99(15):9930–5.

22. Quignon P, Schoenebeck JJ, Chase K, Parker HG, Mosher DS, Johnson GS, et al. Fine Mapping a Locus Controlling Leg Morphology in the Domestic Dog. Cold Spring Harb Symp Quant Biol. 2009 Jan 1;74:327–33.

23. Drögemüller C, Karlsson EK, Hytönen MK, Perloski M, Dolf G, Sainio K, et al. A mutation in hairless dogs implicates FOXI3 in ectodermal development. Science. 2008 Sep 12;321(5895):1462.

24. Cadieu E, Neff MW, Quignon P, Walsh K, Chase K, Parker HG, et al. Coat Variation in the Domestic Dog Is Governed by Variants in Three Genes. Science. 2009 Oct 2;326(5949):150–3.

25. Brown EA, Dickinson PJ, Mansour T, Sturges BK, Aguilar M, Young AE, et al. FGF4 retrogene on CFA12 is responsible for chondrodystrophy and intervertebral disc disease in dogs. Proc Natl Acad Sci. 2017 Oct 24;114(43):11476–81.

26. Plassais J, Rimbault M, Williams FJ, Davis BW, Schoenebeck JJ, Ostrander EA. Analysis of large versus small dogs reveals three genes on the canine X chromosome associated with body weight, muscling and back fat thickness. PLOS Genet. 2017 Mar 3;13(3):e1006661.

27. Millar DS, Lewis MD, Horan M, Newsway V, Easter TE, Gregory JW, et al. Novel mutations of the growth hormone 1 (GH1) gene disclosed by modulation of the clinical selection criteria for individuals with short stature. Hum Mutat. 2003 Apr;21(4):424–40.

28. Mullen MP, Berry DP, Howard DJ, Diskin MG, Lynch CO, Berkowicz EW, et al. Associations between novel single nucleotide polymorphisms in the Bos taurus growth hormone gene and performance traits in Holstein-Friesian dairy cattle. J Dairy Sci. 2010 Dec;93(12):5959–69.

29. Lango Allen H, Estrada K, Lettre G, Berndt SI, Weedon MN, Rivadeneira F, et al. Hundreds of variants clustered in genomic loci and biological pathways affect human height. Nature. 2010 Oct 14;467(7317):832–8.

30. Weedon MN, Lango H, Lindgren CM, Wallace C, Evans DM, Mangino M, et al. Genome-wide association analysis identifies 20 loci that influence adult height. Nat Genet. 2008 May;40(5):575–83.

31. Demerath EW, Guan W, Grove ML, Aslibekyan S, Mendelson M, Zhou Y-H, et al. Epigenome-wide association study (EWAS) of BMI, BMI change and waist circumference in African American adults identifies multiple replicated loci. Hum Mol Genet. 2015 Aug 1;24(15):4464–79.

32. Jiang BJ, Zhan XL, Fu CZ, Wang HB, Cheng G, Zan LS. Identification of ANAPC13 gene polymorphisms associated with body measurement traits in Bos taurus. Genet Mol Res. 2012;11(3):2862–70.

33. White ME, Hayward JJ, Stokol T, Boyko AR. Genetic Mapping of Novel Loci Affecting Canine Blood Phenotypes. PLOS ONE. 2015 Dec 18;10(12):e0145199.

34. Cianfarani S. Insulin-like growth factor-II: new roles for an old actor. Front Endocrinol [Internet]. 2012 Oct 2 [cited 2018 Nov 5];3. Available from: https://www.ncbi.nlm.nih.gov/pmc/articles/PMC3462314/

35. Willer CJ, Sanna S, Jackson AU, Scuteri A, Bonnycastle LL, Clarke R, et al. Newly identified loci that influence lipid concentrations and risk of coronary artery disease. Nat Genet. 2008 Feb;40(2):161–9.

515 36. Kathiresan S, Melander O, Guiducci C, Surti A, Burtt NP, Rieder MJ, et al. Six new loci
516 associated with blood low-density lipoprotein cholesterol, high-density lipoprotein
517 cholesterol or triglycerides in humans. Nat Genet. 2008 Feb;40(2):189–97.

518 37. Li Y, Willer C, Sanna S, Abecasis G. Genotype imputation. Annu Rev Genomics Hum Genet.
519 2009;10:387–406.

520 38. Erbe M, Hayes BJ, Matukumalli LK, Goswami S, Bowman PJ, Reich CM, et al. Improving
521 accuracy of genomic predictions within and between dairy cattle breeds with imputed high-
522 density single nucleotide polymorphism panels. J Dairy Sci. 2012 Jul;95(7):4114–29.

523 39. Yang J, Bakshi A, Zhu Z, Hemani G, Vinkhuyzen AAE, Lee SH, et al. Genetic variance
524 estimation with imputed variants finds negligible missing heritability for human height and
525 body mass index. Nat Genet. 2015 Oct;47(10):1114–20.

526 40. Friedenberg SG, Meurs KM. Genotype imputation in the domestic dog. Mamm Genome.
527 2016 Oct 1;27(9–10):485–94.

528 41. Howie BN, Donnelly P, Marchini J. A Flexible and Accurate Genotype Imputation Method for
529 the Next Generation of Genome-Wide Association Studies. PLOS Genet. 2009 Jun
530 19;5(6):e1000529.

531 42. Browning BL, Browning SR. A Unified Approach to Genotype Imputation and Haplotype-
532 Phase Inference for Large Data Sets of Trios and Unrelated Individuals. Am J Hum Genet.
533 2009 Feb 13;84(2):210–23.

534 43. Shearin AL, Ostrander EA. Leading the way: canine models of genomics and disease. Dis
535 Model Mech. 2010 Jan 1;3(1–2):27–34.

536 44. Li H, Durbin R. Fast and accurate short read alignment with Burrows–Wheeler transform.
537 Bioinformatics. 2009 Jul 15;25(14):1754–60.

538 45. Browning BL, Browning SR. Genotype Imputation with Millions of Reference Samples. Am J
539 Hum Genet. 2016 Jan 7;98(1):116–26.

540 46. McKenna A, Hanna M, Banks E, Sivachenko A, Cibulskis K, Kernytsky A, et al. The Genome
541 Analysis Toolkit: A MapReduce framework for analyzing next-generation DNA sequencing
542 data. Genome Res. 2010 Sep 1;20(9):1297–303.

543 47. DePristo MA, Banks E, Poplin R, Garimella KV, Maguire JR, Hartl C, et al. A framework for
544 variation discovery and genotyping using next-generation DNA sequencing data. Nat
545 Genet. 2011 May;43(5):491–8.

546 48. Van der Auwera GA, Carneiro MO, Hartl C, Poplin R, del Angel G, Levy-Moonshine A, et al.
547 From FastQ Data to High-Confidence Variant Calls: The Genome Analysis Toolkit Best
548 Practices Pipeline. Curr Protoc Bioinforma. 2013;43:11.10.1-11.10.33.

549 49. Delaneau O, Howie B, Cox AJ, Zagury J-F, Marchini J. Haplotype Estimation Using
550 Sequencing Reads. Am J Hum Genet. 2013 Oct 3;93(4):687–96.

551 50. Howie B, Fuchsberger C, Stephens M, Marchini J, Abecasis GR. Fast and accurate genotype
552 imputation in genome-wide association studies through pre-phasing. Nat Genet. 2012
553 Aug;44(8):955–9.

554 51. Perez F, Granger BE. IPython: A System for Interactive Scientific Computing. Comput Sci
555 Engg. 2007 May;9(3):21–29.

556 52. Hunter JD. Matplotlib: A 2D Graphics Environment. Comput Sci Eng. 2007 May;9(3):90–5.

557 53. Purcell S, Neale B, Todd-Brown K, Thomas L, Ferreira MAR, Bender D, et al. PLINK: A Tool
558 Set for Whole-Genome Association and Population-Based Linkage Analyses. Am J Hum
559 Genet. 2007 Sep 1;81(3):559–75.

54. Zhou X, Stephens M. Genome-wide Efficient Mixed Model Analysis for Association Studies. Nat Genet. 2012 Jun 17;44(7):821–4.

55. Li M-X, Yeung JMY, Cherny SS, Sham PC. Evaluating the effective numbers of independent tests and significant p-value thresholds in commercial genotyping arrays and public imputation reference datasets. Hum Genet. 2011 Dec 6;131(5):747–56.

56. R Core Team. R: A Language and Environment for Statistical Computing. [Internet]. Vienna, Austria: R Foundation for Statistical Computing; 2013. Available from: http://www.R-project.org/

57. Venables WN, Ripley BD. Modern Applied Statistics with S. Fourth edition. New York: Springer; 2002.

58. Cingolani P, Platts A, Wang LL, Coon M, Nguyen T, Wang L, et al. A program for annotating and predicting the effects of single nucleotide polymorphisms, SnpEff. Fly (Austin). 2012 Apr 1;6(2):80–92.

59. Campbell CL, Bhérer C, Morrow BE, Boyko AR, Auton A. A Pedigree-Based Map of Recombination in the Domestic Dog Genome. G3 GenesGenomesGenetics. 2016 Sep 2;6(11):3517–24.

Figures:

Figure 1: Imputation accuracy for 33,144 variants of different allele frequency in mixed-breed dogs (blue), purebred dogs (green), and village dogs (red).
a) all sites, b) heterozygous sites only.

Figure 2: Scatter plots showing *P*-values for array GWAS (x axis) and imputed GWAS (y axis).

583 a) breed-average weight, b) breed-average height, c) individual weight, and d) absolute values of
584 the effect sizes of the most-associated SNP for breed-average weight and breed-average height
585 from the imputed GWAS.
586
587 Figure 3: Novel body size loci.
588 Linkage disequilibrium plots of the region around breed-average weight GWAS results
589 a) CFA9:12, b) CFA26:7. Array genotypes are shown as o, imputed data are shown as +. Colors
590 indicate amount of LD with the most significantly associated SNP, ranging from black (r^2<0.2) to
591 red (r^2>0.8).
592
593 Figure 4: Stepwise-covariate LD plots for breed-average weight imputed GWAS.
594 a) CFA7 (*SMAD2*), showing that the association signal in the region disappears with the inclusion
595 of the top 4 SNPs as covariates. b)-d) Association signal in the region remains with the inclusion
596 of the top 4 SNPs as covariates and then additional stepwise covariates in the region b) *LCORL*,
597 c) *HMGA2*. Array genotypes are shown as o, imputed data are shown as +. Colors indicate
598 amount of LD with the most significantly associated SNP, ranging from black (r^2<0.2) to red
599 (r^2>0.8).
600
601 Figure 5: LD plots for significant blood phenotypes.
602 a) albumin on CFA13, b) anion gap on CFA29, c) calcium on CFA37, d) sqrt glucose on CFA1, e)
603 potassium on CFA8, f) white blood cells on CFA4, g) log ALT on CFA13, h) sqrt amylase on
604 CFA6. Array genotypes are shown as o, imputed data are shown as +. Colors indicate amount of
605 LD with the most significantly associated SNP, ranging from black (r^2<0.2) to red (r^2>0.8).
606
607 **Supporting Information:**
608 S1 Figure: Linkage Disequilibrium (LD) plots of the region around the breed-average weight QTL
609 intervals that have been fine-mapped a) CFA3:41 near the gene *IGF1R*, b) CFA4:39 near the
610 gene *STC2*, c) CFA4:67 near the gene *GHR*, d) CFA7:43 near the gene *SMAD2*, e) CFA10:8

near the gene *HMGA2*, f) CFA15:41 near the gene *IGF1*, g) CFA18:20, h) CFA32:5 near the gene *BMP3*, i) CFAX near the gene *IGSF1*. Dashed lines show the significant interval (defined by *P*-values within two orders of magnitude of the most associated SNP). Asterisks show the location of the causal locus. Note that for d), f), and g) the causal locus is a deletion, SINE insertion, and retrogene insertion respectively, so these locations are labeled with asterisks at the top of the plot.

S2 Figure: Linkage Disequilibrium (LD) plots of the region around the breed-average weight QTL intervals on a) CFA3:91 near the gene *LCORL* and *ANAPC13*, b) CFA7:30 near the gene *TBX19*. The significant interval, drawn with dashed vertical lines, is defined by *P*-values within two orders of magnitude of the most associated SNP. Array genotypes are shown as o, imputed data are shown as +. Arrows point to the most significant SNP in the array GWAS and imputed GWAS. Colors indicate amount of LD with the most significantly associated SNP, ranging from black (r^2<0.2) to red (r^2>0.8).

S1 Table: Imputation accuracy calculated for each chromosome for village dogs, mixed-breed dogs, and purebred dogs. Average recombination rate (cM/Mb) calculated from (59) for each chromosome is also shown.

S2 Table: *P*-values for body size GWAS QTLs using individual weight, breed-average weight, and breed-average height phenotypes with array genotypes and imputed panel. Novel body size loci are shown in bold.

S3 Table: Significant and nearly significant imputed GWAS results of blood phenotypes. Also shown is the location and *P*-value from the GWAS using the array genotype data.

S4 Table: List of Whole Genome Sequence (WGS) dog samples.

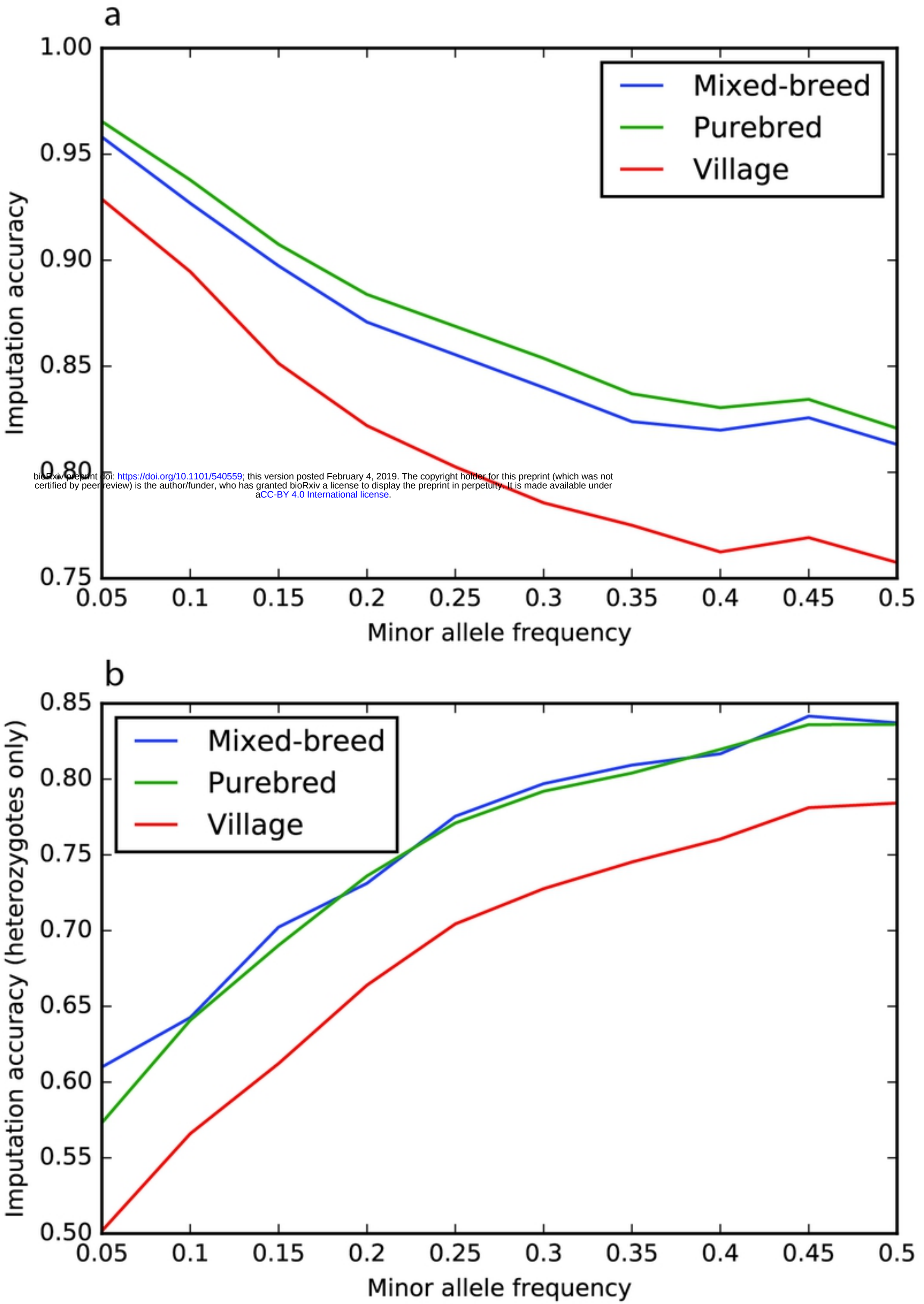

Figure 1

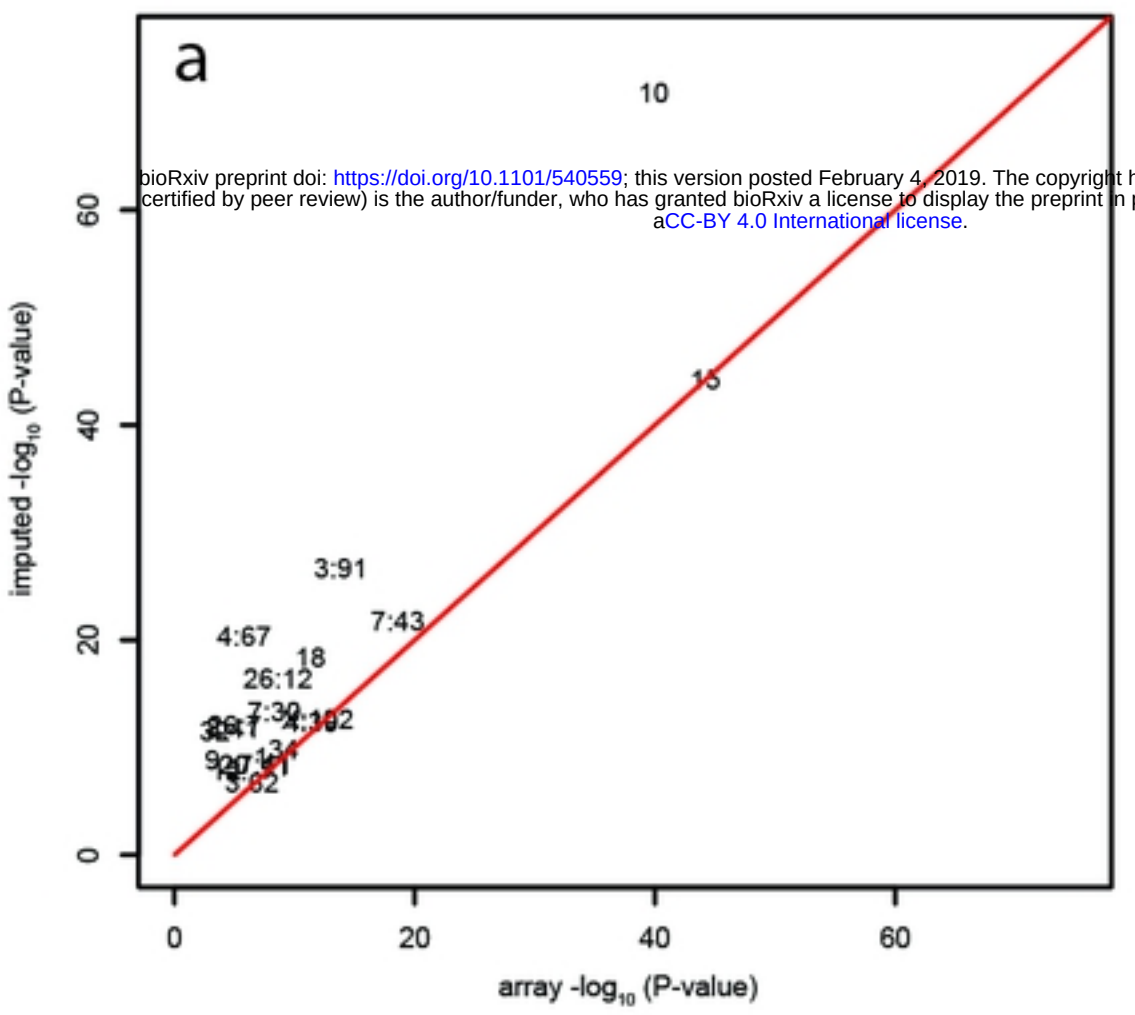

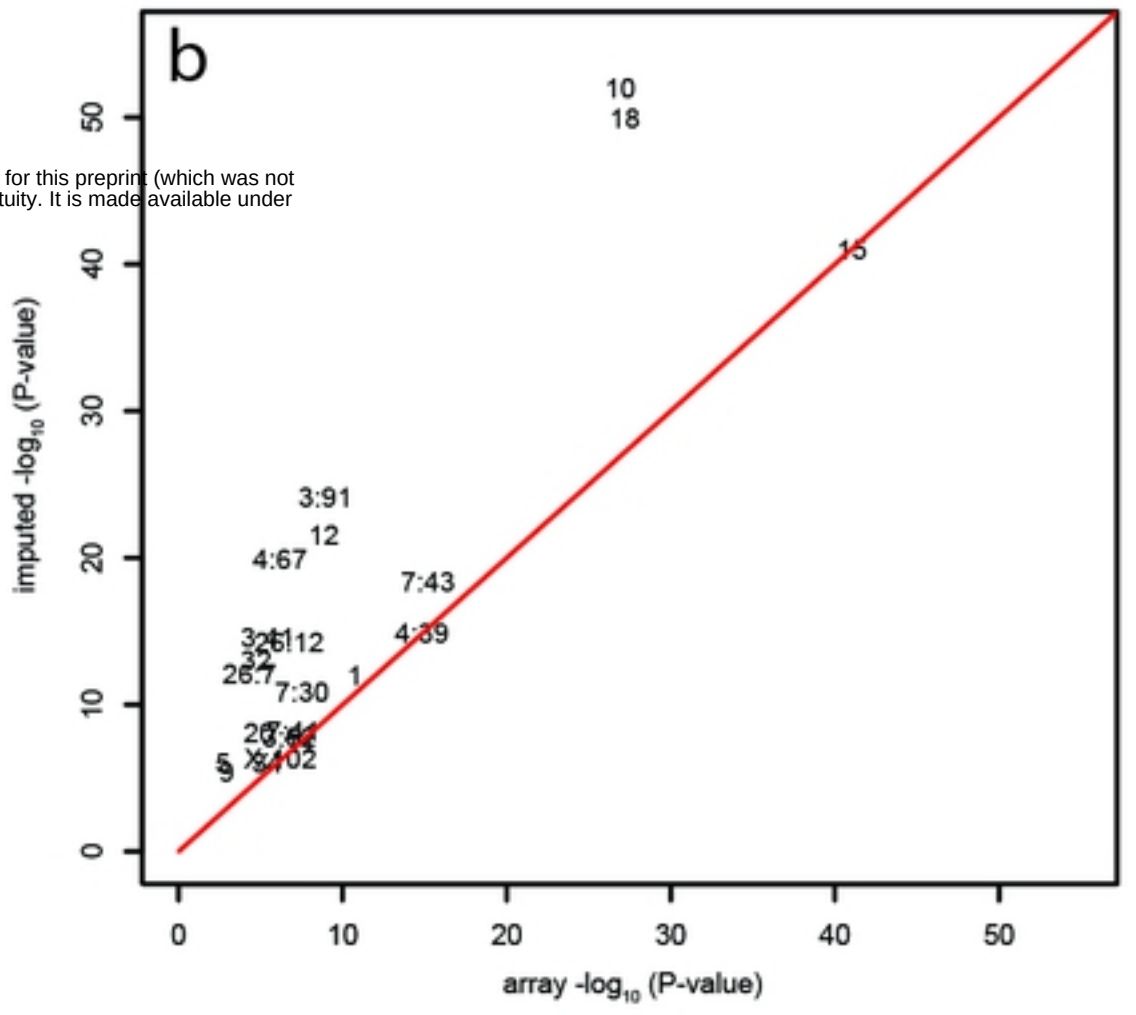

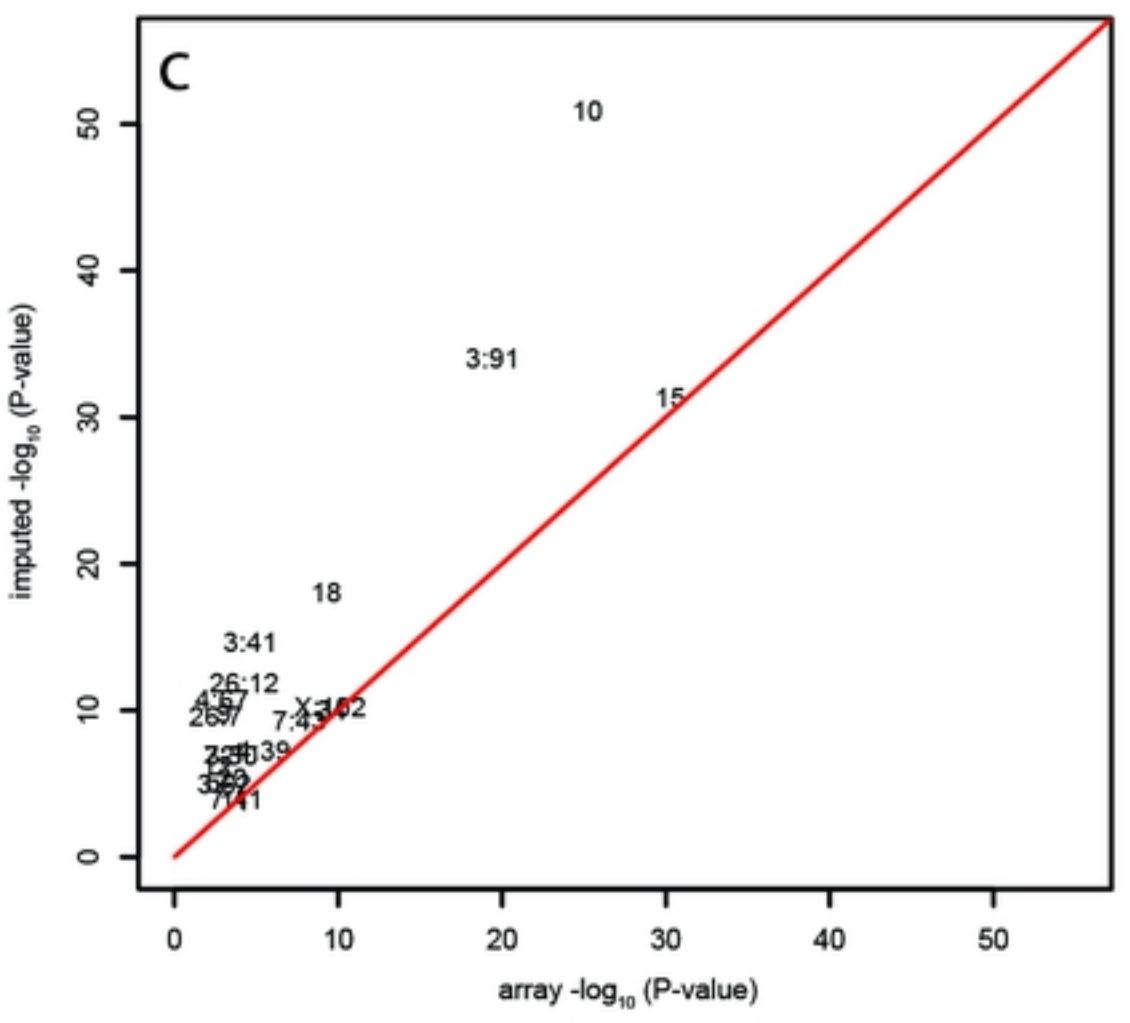

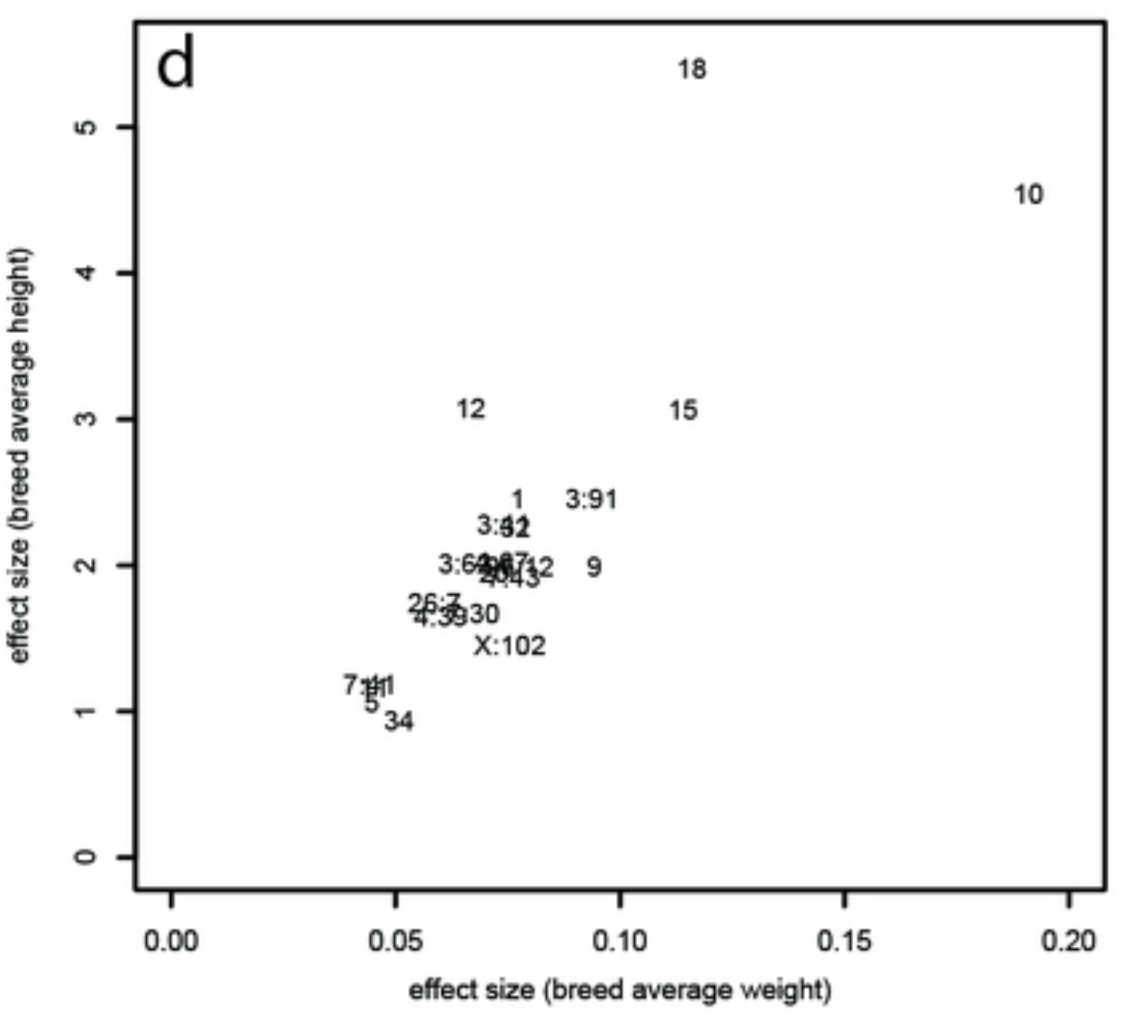

Figure 2

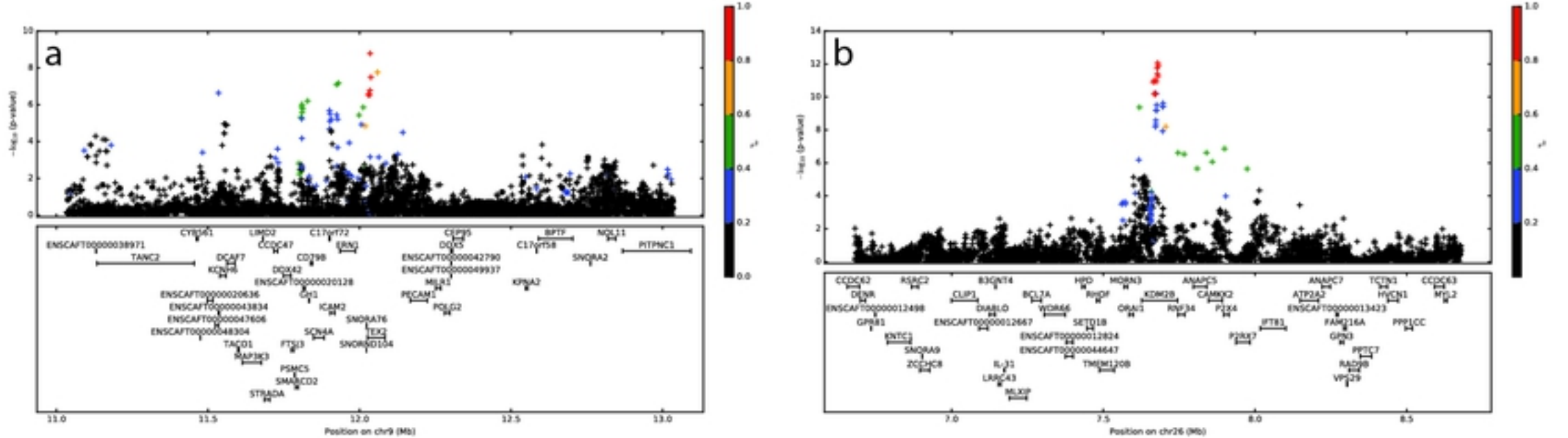

Figure 3

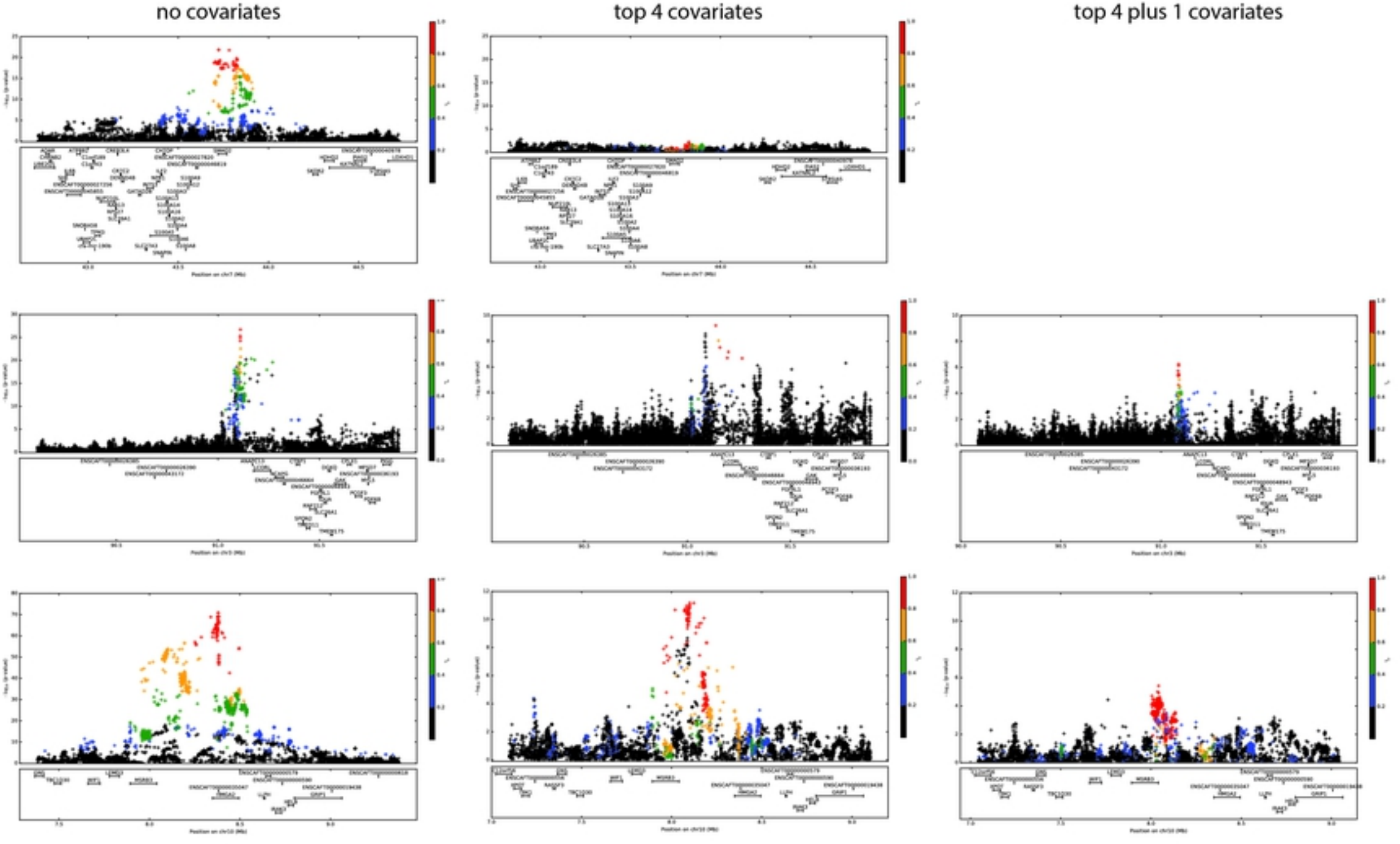

Figure 4

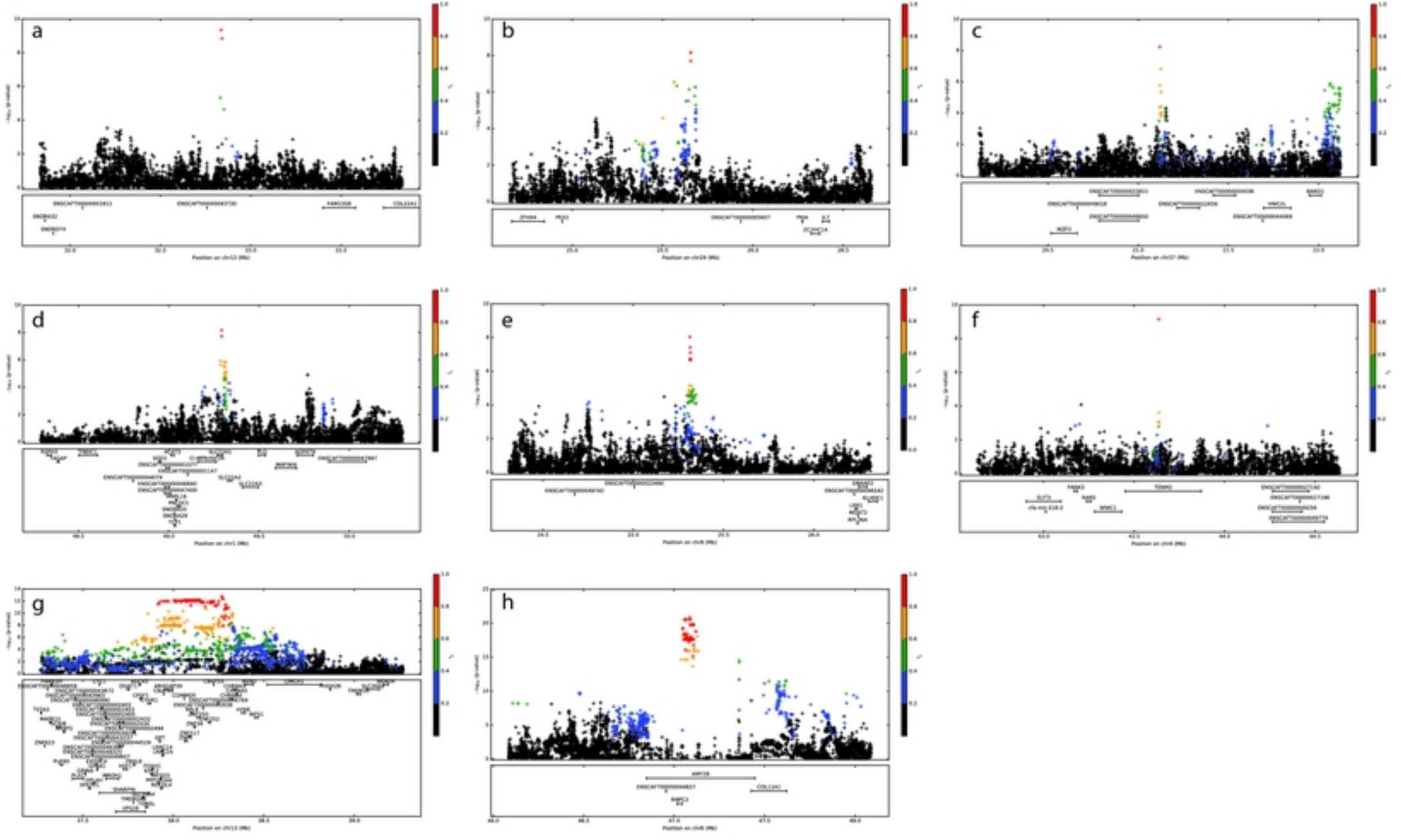

Figure 5